ACS EARTH AND SPACE CHEMISTRY

Article

Cite This: ACS Earth Space Chem. 2019, 3, 1955−1965

http://pubs.acs.org/journal/aesccq

# Physicochemical Properties and Complexity of Amino Acids beyond Our Biosphere: Analysis of the Isoleucine Group from Meteorites

Fabiana Da Pieve*

Royal Belgian Institute for Space Aeronomy, BIRA-IASB, Brussels, Belgium

Supporting Information

**ABSTRACT:** Understanding the physicochemical properties of biomolecules and how these properties drive the emergence of complexity in the assembly/condensation of such systems is important for understanding a variety of reactions taking place in astrophysical environments, in particular those where polymerization processes occur on mineral surfaces or solid organic matter form in cold-chemistry processes. Here, a computational study of the structural and electronic properties of the gas and condensed phases of the isoleucine group of amino acids, found with large enantiomeric excess in Antarctic meteorites, is presented. An analysis of a *statistical complexity* measure related to their electronic properties, of the degree of chirality, and of the H-bond patterns is also reported. The results, based on Density Functional Theory, Many Body Perturbation Theory, and Møller−Plesset perturbation theory, show that a) the condensed amino acids keep reminiscence of structural and electronic properties of the gas phase molecules, b) the proteinogenic L-isoleucine gains in complexity and chirality upon condensation, contrary to its diastereomer, which is absent in living systems, and c) the complexity based on electronic properties can contrast with the notion of structural/geometrical complexity. The findings suggest that future scoring strategies of organic molecules should rely on both structural/geometrical molecular complexity and on the electronic properties, which in different states of matter are determined by other degrees of freedom (configurational or chiral) to a different extent, as well as on information storage capability of self-assembly configurations constrained by an atomistic chemistry perspective.

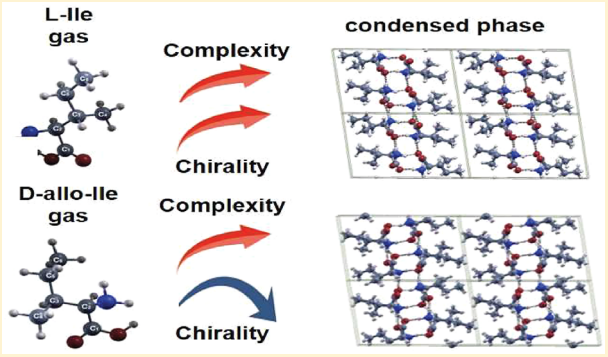


**KEYWORDS:** *aliphatic amino acids, meteoritic organics, isoleucine, density functional theory calculations, many body perturbation theory, electronic properties, chirality*

## INTRODUCTION

The recent observations of water ice in the shallow subsurface of Mars[1] and liquid water and active geology on Jupiter's moon Europa[2] and Saturn's moon Enceladus,[3] point at a large diversity of environments in the Universe that could host or could have hosted life. Life forms could emerge starting from different states of organic matter and eventually develop in different solvents. A still unanswered question is how to estimate the complexity of prebiotic or biomolecules encountered in such possibly very diverse environments, and, ultimately, how to recognize life.

Being the building units of proteins, amino acids are high priority targets in the search for life elsewhere in the Universe,[4] either as gas phase molecules in planetary/small bodies atmospheres or as solid organic matter. The latter can be expected in the crust of jovian icy moons, at surface brines[5] and evaporite deposits[6] on Titan's surface, or within the aerosols of its atmosphere,[7] and at Enceladus surface[8] or within the icy grains of its plumes.[9,10] Rich solid-phase chemistry leading to amino acids and relevant prebiochemicals is also triggered by irradiation in astrophysical[11−14] and cometary ices,[15] by mobile reactants in growing ice mantles of dust grains[16] and by shock-induced reactions in collisions of icy grains.[17] Formation of condensed amino acids in cold environments is also suggested by findings of amino acids in pristine Antarctic meteorites.[18] This, combined with the preferred handedness of amino acids in meteoritic samples,[19−21] points to the possibility that condensation phenomena might have influenced the chiral assembly of solid organic matter.[22−25] Nevertheless, meteoritic samples exhibit a very large set of amino acids, most of them unknown to our biosphere,[26−29] which suggests that amino acids cannot be considered as unambiguous indicators of life.

Current strategies for biosignature detection rely mainly on established features associated with life on Earth, as specific classes of molecules, isotopic signatures, molecular weights patterns of fatty acids or other lipids, and enantiomeric excesses. Different directions are under investigation nowadays to unravel possible universal features of life, especially in

Received: May 11, 2019
Revised: July 3, 2019
Accepted: July 19, 2019
Published: July 19, 2019






DOI: 10.1021/acsearthspacechem.9b00131
ACS Earth Space Chem. 2019, 3, 1955−1965

connection with research on exoplanets.[30] From the molecular point of view, analysis of general binding patterns for different chemical data sets[31] and complexity-scoring scales[32,33] have been proposed. The latter are put forward on the basis of molecular complexity, as indicator of the structure of the single molecules, and of the Shannon's information content[34] of the sequence formed by such molecules, i.e., the degree of randomness (or variability) of their microscopic arrangements giving the global pattern. However, the electronic properties of the building blocks on which the biomolecular machinery of life is based, as we know it, also play a fundamental role and the information storage capability of the self-assembly of such building blocks can well be constrained by real atomistic chemistry. Several recent works have highlighted the role of physicochemical properties in allowing for optimal covering of the chemical space in terms of size, hydrophobicity, and charge,[35] in determining energy input−dissipation mechanisms, storing energy in bonds,[36] in driving energy dissipation and self-organization of structures,[37] and in determining a universal charge transport mechanism via a specific arrangement of the highest occupied molecular orbital (HOMO) and of the lowest unoccupied molecular orbital (LUMO).[38,39] Also, the electronic properties have been shown to play a relevant role in the modern diversification of amino acids,[40] as well as in satisfying specific H-bond requirements for life.[41] Previous works[42,43] have evaluated the complexity of the electronic properties for known amino acids via the statistical complexity measure from López-Ruiz−Mancini−Calbet[44,64] ($C_{LMC}$ complexity), which is based on both the Shannon entropy of the electronic distribution (describing its randomness) and the disequilibrium of such distribution (i.e., its distance from a uniform distribution). Others have used information-based descriptors of the electronic properties to study the chirality and similarity between mirror images (enantiomers) of chiral molecules.[45−48] Studies of complexity measures for condensed phases are scarce and deal with inorganic systems with focus on the sole structural complexity.[49]

Given the large diversity of environments of interest for astrochemistry and meteoritic studies, it is opportune to investigate such paradigm shift toward information theory also to explore the emergence of complexity in the electronic properties of amino acids in different states of matter. In this context, here a computational study of the structural, electronic, and chiral properties, H-bond patterns, and the statistical complexity related to the electronic properties is presented, for both the gas and condensed phase of a specific group of meteoritic amino acids recently found in Antarctic meteorites with large enantiomeric excess.[18] The $\alpha$-amino acids from the isoleucine series [2-amino 3-methylpentanoic acid, $CH_3CH_2-CH(CH_3)-CH(NH_2)-COOH$], either involved in protein synthesis, in human plasma, or not present in living systems, are considered. Calculations are performed at the density functional theory (DFT) level and at the many body perturbation theory approach (MBPT) for the condensed phases and MP2 perturbation approach level for the gas phase amino acids. The results show that the electronic properties of the amino acids in the condensed phase are indicative of a higher propensity to chemical reactivity, potentially allowing for a higher complexification of the system, that complexity and chirality change according to the state of matter, and that the complexity measure based on electronic properties can contrast with the intuitive notion of structural complexity.

## METHODS

**Isoleucine Series.** Isoleucine contains two chiral carbons ($C_\alpha$,$C_\beta$) and exists as two distinct compounds based on the spatial orientation of the two substituents at those carbons (Figure 1). The isomer having absolute configuration *S* at both

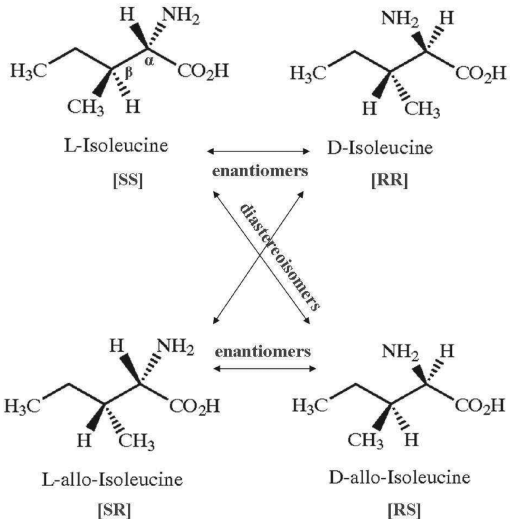


**Figure 1.** Representation of the two enantiomers L-Ile and D-Ile (where change of chirality occurs at both the $C_\alpha$ and $C_\beta$ atom) and their diastereomers D-allo-Ile and L-allo-Ile (which exhibit change of chirality only at one chiral carbon center).

chiral carbons ([*S*,*S*]) is the naturally occurring $\alpha$-amino acid L-isoleucine (L-Ile), used for the proteins synthesis. Its mirror image amino acid (enantiomer) is the [*R*,*R*] isomer D-isoleucine (D-Ile), not shown in our life. L-Ile transforms to its diastereomer D-allo-isoleucine via $\alpha$-epimerization, following loss and acquisition of protons on opposite sides of the molecule and chiral reversal only at the $\alpha$-carbon, known also as $C_2$. D-Allo-isoleucine (D-allo-Ile, with configuration [*R*,*S*]) is also not found in living organisms.[18,50] The enantiomer of the latter is L-allo-isoleucine (L-allo-Ile, with [*S*,*R*] configuration at the two chiral carbons), not involved in protein biosynthesis but featured in bacteria, fungi, and plants and human plasma.

In the solid, as in the liquid phase, isoleucine is in its zwitterionic state, i.e., the $\alpha$-amino group is protonated $-NH_3^+$ and the $\alpha$-carboxylic acid group is deprotonated $COO^-$. The four stereoisomers of isoleucine assemble in several different condensed phases.[51,52] Here the pure enantiomeric crystal of L-Ile (with the observed $Z' = 2$ packing determined by glide planes[53] and the energetically close $Z' = 1$ packing, crystallyzing with only one molecole in the asymmetric unit), the pure enantiomeric crystal of D-allo-Ile, the racemic LD-Ile, and the diastereomeric complex D-Ile:D-allo-Ile are considered. Allo-Ile spontaneously resolves in its enantiomers, forming a conglomerate crystal,[51] while Ile forms racemate crystals (LD-Ile). The initial crystal structures were taken from the Cambridge Structural Database, except the (unusual) structure of L-Ile $Z' = 1$, kindly provided by Prof. G. M. Day from Univ. of Southampton, UK. In a previous study,[52] it was shown that the condensation of L-Ile does not significantly benefit from a $Z' = 2$ packing with respect to a $Z' = 1$ structure (with actually two $Z' = 1$ structures found slighly more stable than the observed $Z' = 2$ one), and thus, an investigation of the electronic properties of the latter has also been performed. For


DOI: 10.1021/acsearthspacechem.9b00131
ACS Earth Space Chem. 2019, 3, 1955−1965

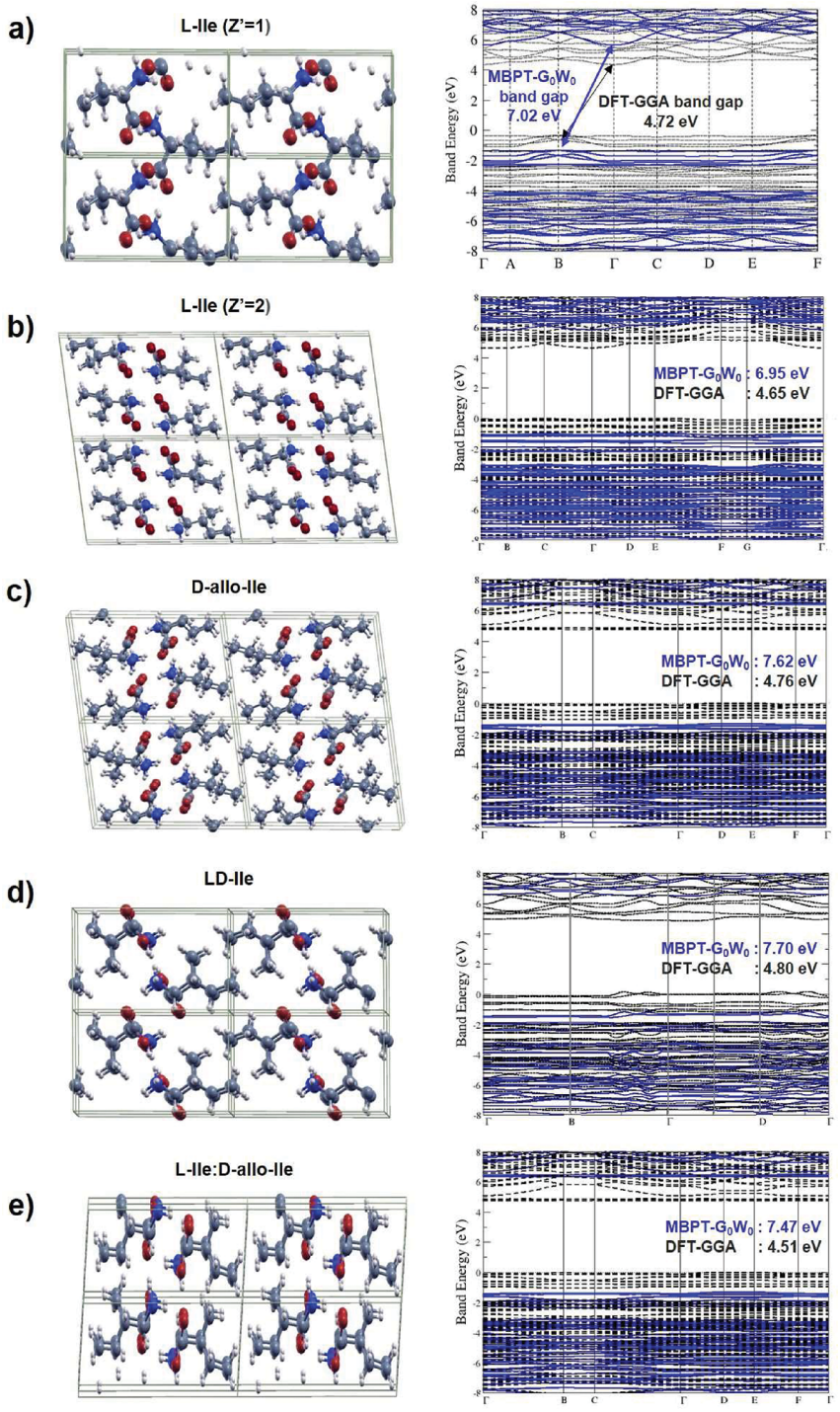


**Figure 2.** Optimized crystal structures, visualized as 2 × 2 × 2 supercells. From top to bottom: (a) L-Ile ($Z'$ = 1), (b) L-Ile ($Z'$ = 2), (c) D-allo-Ile, (d) LD-Ile, and (e) L:Ile:D-allo-Ile. Corresponding band structures are also shown (obtained with Wannier interpolation at the DFT-GGA (black) and $G_0W_0$ level (blue)).

the gas phase molecules, the initial geometries of L-Ile and D-allo-Ile have been taken from the PubChem database.

**Computational Details.** *Structural and Electronic Properties.* A hierarchy of electronic structure approaches is used in this work for both the condensed structures and the gas phase amino acids (and the molecular units "frozen" in the condensed phases). Geometry optimization of both the condensed and gas phase amino acids was performed at the DFT-hybrid Becke three-parameter Lee−Yang−Parr (B3LYP)[54,55] level with tight self-consistent criteria. For the condensed phases, calculations were performed using periodic boundary conditions within the plane-wave code VASP,[56] with Projector Augmented Wave (PAW) potentials,[57] with a large basis with a cutoff of 900 eV. A preliminary optimization with the Generalized Gradient Approximation (GGA) in the Perdew−Burke−Ernzerhof parametrization,[58] taking into account the van der Waals (vdW) interactions via the DFT+D2 approach[59] was performed before the one with B3LYP. Further details on the *k*-mesh for reciprocal space and on the optimization procedure are described in the Supporting



DOI: 10.1021/acsearthspacechem.9b00131
ACS Earth Space Chem. 2019, 3, 1955−1965

Information (SI). For the optimization of gas phase molecules, calculations were performed with the 6-311++G(d,p) basis set using the Gaussian09 code.[60] For the molecular units extracted from the solid, a solvation has been performed to keep the charge distribution for the zwitterionic configuration, using a PCM model[61] (see SI for details), keeping rigid the molecular conformation as extracted from the solids.

The band gaps for the condensed systems and the HOMO−LUMO gaps for the molecular units (both the gas phase amino acids and those extracted from the condensed phases) have been calculated, respectively, by applying Many Body Perturbation Theory (MBPT) (in the so-called $G_0W_0$ approximation) and second-order Møller−Plesset (MP2) theory, starting from the previously optimized structures at DFT-B3LYP level. An important quantity that is used extensively to make predictions on the stability of a molecule is the hardness[62] $\eta = \frac{\mathrm{IP} - \mathrm{EA}}{2}$, where IP is the ionization potential (energy necessary to remove an electron a neutral atom or molecule) and EA the electron affinity (energy necessary to add an electron to a neutral atom or molecule to form a negative ion/negatively charged molecule). The hardness is actually related to the HOMO−LUMO gap in simple molecular orbital theory since IP can be considered as the negative of the HOMO and EA the negative of the LUMO (actually, a generally applicable linear correlation relationship exists between the calculated HOMO/LUMO energies and the experimental/calculated IPs/EAs[63]). Larger values of $\eta$ (and of the HOMO−LUMO gap) correspond to less reactive molecules.

*Complexity and Chirality.* The López-Ruiz, Mancini, and Calbet[64] complexity, denoted as $C_{LMC}$, is given by the product of two entropy measures:

$$C_{LMC} = D[\rho]\mathrm{e}^{S[\rho]} = D[\rho]L[\rho] \tag{1}$$

i.e., the disequilibrium $D[\rho]$, which quantifies the departure of the probability density from uniformity:

$$D[\rho] = \int \rho^2(\vec{r})\, \mathrm{d}\vec{r} \tag{2}$$

and $L[\rho] = \mathrm{e}^{S[\rho]}$, which involves the Shannon entropy $S[\rho]$. The latter quantifies the departure of the probability density from localizability (and thus it is a general measure of randomness of the probability density):

$$S[\rho] = -\int \rho(\vec{r}) \ln \rho(\vec{r})\, \mathrm{d}\vec{r} \tag{3}$$

($\rho(\vec{r})$ is the probability density, normalized to unity). In relation to the electronic distribution, $S$ gives information on the variability of the information string needed to describe the delocalization of the electronic cloud. For discrete variables, a simple example can be found in the Petz's book:[65] if we want to pass the information on the name of the winning horse in a race with 8 horses, where all horses have the same propability to win, the minimum length of a message is given by $S = \sum_{i=1,8} \frac{1}{8} \log_2 \frac{1}{8} = 3$. This means that each horse can be identified with a message expressed by a combination of 1s and 0s of length 3 (3 bits). The Shannon entropy does not say anything about the properties that identify each horse (e.g., the color, age, etc.); such characteristics are communicated via the encoding process (a string of 0s and 1s). The complexity $C_{LMC}$ has been calculated on both the gas phase amino acids and on the molecular units "frozen" in the condensed matrices, via home-based developed routines along with multidimensional integration routines[66] combined with spline interpolations of the electron density functions $\rho(\vec{r})$, partially reusing some parts of the BRABO package.[67] A fine grid spacing was used, assuring integration accuracy (see SI).

The chirality index considered in this work is the Avnir's Continuous Chirality Measure (CCM), which can be calculated via the freely available tool by the Avnir's group (http://www.csm.huji.ac.il/new/), once the files with the coordinates of the gas phase amino acids and of the molecular units extracted from the condensed phases are uploaded. This quantity is based on the distance of a chiral object from the closest abstract achiral one. The algorithm evaluates quantitatively the degree of chirality in a range from 0—the molecule corresponds to an achiral object—to higher values (the upper limit is 100)—expressing the distance from the closest achiral object:[68]

$$S(G) = \frac{1}{n} \sum_{i=1}^{n} ||P_i - \hat{P}_i||^2 \tag{4}$$

where $G$ is a given symmetry group, $P_i$ are the points of the original configuration, $\hat{P}_i$ are the corresponding points in the nearest $G$-symmetric configuration, and $n$ is the total number of configuration points. Thus, the algorithm finds the set of points $\hat{P}_i$, which possesses the desired symmetry ($G$ symmetry), such that the total normalized distance from the original shape $P_i$ is minimal. The algorithm screens $S$ over the symmetry groups having a reflection mirror, an inversion center, or a higher order improper rotation axis, which are indeed possessed by achiral objects.

## RESULTS AND DISCUSSION

**Structural and Electronic Properties: Changes upon Condensation/Sublimation.** The relaxed structures of the condesed phases obtained by a B3LYP (re)optimization (on top of the preliminary GGA+D2 calculation) are shown in Figure 2 (represented as 2 × 2 × 2 supercells to favor visualization). The geometric parameters obtained are in good agreement with the available experimental parameters (see SI). The different condensed phases are all found relatively close in energy, with the most stable structure being the racemic LD-Ile, in line with previous works,[52] followed by D-allo-Ile and the diastereomeric complex L-Ile:D-allo-Ile. D-Allo-Ile is more stable than L-Ile, with a gain in energy of 6.28 kcal/mol with respect to the $Z' = 2$ structure of L-Ile, which is found to be more stable than the $Z' = 1$ structure of L-Ile, in line with previous works.[69] D-Allo-Ile crystallizes with two independent and dissimilar molecules in the elementary cell,[51,70] which have different side-chain conformations: in molecule A, the torsion angle defining orientations about the C−C bonds in the side groups ($N-C_2-C_3-C_5$) is *trans*, while molecule B is *gauche*$^-$. The conformation of the molecules is found to be similar in the different crystals. The conformation of L-Ile is the $Z' = 2$ structure, similar to the one in the structure of LD:Ile and L-Ile:D-allo-Ile, confirming previous results.[51] The conformation of D-allo-Ile in the pseudoracemate L-Ile:D-allo-Ile corresponds to that of one of the two molecular units (unit A) in the enantiomerically pure D-allo-Ile structure.

The optimized gas phase amino acids and the two molecular units (A and B) with which the two enantiomerically pure crystals L-Ile ($Z' = 2$) and D-allo-Ile condense are reported in Figure 3. The gas phase D-allo-Ile is found to be (slightly)


DOI: 10.1021/acsearthspacechem.9b00131
ACS Earth Space Chem. 2019, 3, 1955−1965

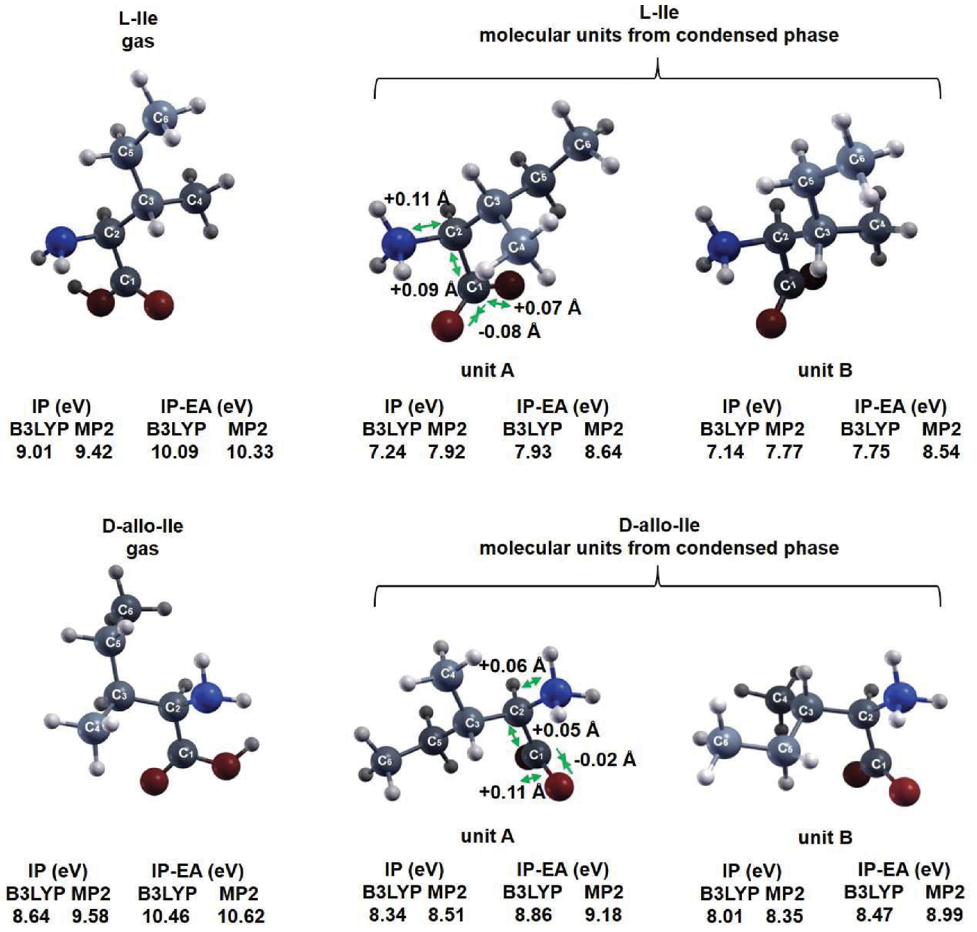


**Figure 3.** Top row: L-Ile in the gas phase and the (zwitterionic) molecular units A and B extracted from the condensed phase ($Z' = 2$). Bottom row: D-allo-Ile in the gas phase and the (zwitterionic) molecular units A and B extracted from the condensed phase. Arrows indicate the stretching or shortening of the bonds upon condensation (the same behavior is also valid for the units B, where the differences in bond length with the gas phase molecule vary at maximum of 0.01 Å) w.r.t. unit A.

more stable than L-Ile (by 0.43 kcal/mol), following the trend of the condensed phases, but in contrast with previous results.[71] Actually, in both works the energy difference is at the limit of the accuracy of the methods; the results obtained here, however, hint to a reminiscence of stability upon phase-change, similarly to what occurs for the structural and electronic properties as discussed below. For L-Ile, a slightly higher stability for the isomer bearing a single hydrogen bonding between the hydroxyl hydrogen and the amino nitrogen O−H−$NH_2$ w.r.t. the isomer with a bifurcated hydrogen bonding from the amide to carbonyl groups $NH_2$−O═C is found (see SI), in agreement with other MP2[72,73] and B3LYP/6-311+G(d,p) results,[74] although in contrast with other MP2/6-311++G(d,p)[75] and B3LYP/6-31G(d,p)[76] calculations. In Figure 3, arrows indicate the shortening and stretching of bonds, which occurr in both L-Ile and D-allo-Ile, and numbers are the differences in bond length with respect to the gas phase molecule. The skeletal structure of the gas phase amino acids is almost preserved upon condensation, with most of the C−C bonds left unaltered, in agreement with previous works.[77] Some changes occur only for specific bonds. In particular, while in the gas phase the C═O bond is shorter than the C−O bond and has a greater population reflecting the double nature of the bond, these two bonds acquire approximately the same length upon condensation, as already observed in a previous study.[78]

Figures 2 and 3 also report respectively the dispersion of the electronic states (and band gaps) in the condensed phases and the IP and IP-EA distance (reflecting the HOMO−LUMO gap) for both the gas phase amino acids and the molecular units extracted from the condensed phases. The results from Figure 2 show that (a) the dispersion of the electronic states in the condensed phases show nearly no dispersion, which implies highly localized states reminiscent of those of individual molecules and is the reason why many spectroscopic measurements in molecular crystals have often been explained by using the spectra of the individual molecules;[79−81] (b) the differences between the band gap of the experimentally observed L-Ile $Z' = 2$ structure and of the L-Ile $Z' = 1$ are at the limit of computational accuracy, and that the dispersion of conduction states appears as the main difference between such two phases; (c) the condensed amino acids are all found to be wide gap semiconductors at the $G_0W_0$ level, similarly to previously analyzed amino acids,[78,82,83] with D-allo-Ile having larger band gap with respect to L-Ile. The result in Figure 3 on the IP at MP2 level for the gas phase L-Ile (9.42 eV) matches reasonably well the experimental value for the conformer here studied (9.57 eV[84]) and previous results from MP2 (9.77 eV[72]) or the Outer Valence Green's function (OVGF) method (9.65 eV,[76] 9.85 eV[74]). Agreement is also observed at DFT level between the B3LYP value obtained here, 9.01 eV, and the previous result of 9.18 eV in ref 73. The results in Figure 3 tell


DOI: 10.1021/acsearthspacechem.9b00131
ACS Earth Space Chem. 2019, 3, 1955−1965

that the zwitterionic molecular units in the solid state, which thus have a more similar configuration to the one in a liquid physiological solution, have smaller HOMO−LUMO gaps with respect to the gas phase amino acids, and thus higher reactivity and polarizability, since the electron distribution can be distorted readily if the LUMO energy lies close to the HOMO energy. This implies that the formation of larger biomolecules and the potential complexification of the system might be more favored in solid organic matter. For the zwitterionic units of L-Ile extracted from the condensed phase, the IPs are in reasonable agreement with the 8.00 eV value for the amino acid in solution.[72] Last, by looking at the band gaps in Figure 2 and at the IP−EA distances in Figure 3, we see that the higher band gap of the condensed D-allo-Ile with respect to L-Ile recalls the results on the HOMO−LUMO gaps of both the corresponding gas phase amino acids and the molecular units extracted from the solids.

The higher abundancy of D-allo-Ile with respect to L-Ile in highly pristine CR2.6 chondrite meteorites,[18,85] accompanied by the largest ever reported enantiomeric excess of a nonprotein amino acid, can be related in this study to the energetics of D-allo-Ile following structural optimization, its higher HOMO−LUMO gap (suggesting a lower propensity to reactivity), and the spontaneous resolution of allo-Ile in conglomerate crystals (separate enantiomerically pure crystals) reported in previous works.[51] Also, the larger band gap of D-allo-Ile with respect to L-Ile suggests less reactivity to secondary light projectiles generated in the track of energetic galactic cosmic rays,[12] as the response to irradiation by the electronic degrees of freedom suddenly decreases for systems with large band gap, when the projectiles have slowed down.[86]

It is important to note that, for the gas phase and the molecular units extracted from the condensed phases, the higher level MP2 results do not change the ordering of the HOMO−LUMO gaps found at B3LYP level. Such sequence ordering kept at different levels of theory gives confidence that the complexity $C_{LMC}$ can reasonably be estimated on the basis of the electronic properties at the B3LYP level. Also, a recent study on the evaluation of the (atomic) Shannon entropy has recently shown that B3LYP behaves averagely well in the calculation of such quantity.[87]

**Complexity and Chirality Indexes: Changes upon Condensation/Sublimation.** In Figure 4, the complexity $C_{LMC}$ and the chirality index CCM are plotted vs IP−EA for both the gas phase amino acids and the molecular units extracted from the condensed phases. Given the different approximations used, and the optimization at different level of theory, the agreement for L-Ile (gas) with previous results obtained at the MP2 level ($C_{LMC} \approx 15.0-15.2$ au for Ile[42]) is fair. It is observed that the zwitterionic molecular units have higher complexity $C_{LMC}$, to0gether with a lower HOMO−LUMO gap as discussed above, with respect to the gas phase amino acids.

About chirality, as L-Ile and D-allo-Ile are not enantiomers but diastereomers, their chirality index obviously differs. For the mirror image of L-Ile, as extracted from the racemic system LD-Ile, the chirality degree is identical to the L-Ile molecular unit in the system (within the level of computational errors, i.e., 12.428 and 12.429, respectively). The value obtained for gas phase L-Ile (7.43) is in reasonable agreement with the 7.73 value reported in previous works,[88] obtained with the same functional (B3LYP) but a different basis set (6-31G(d,p)). Both enantiomerically pure solids crystallize with two

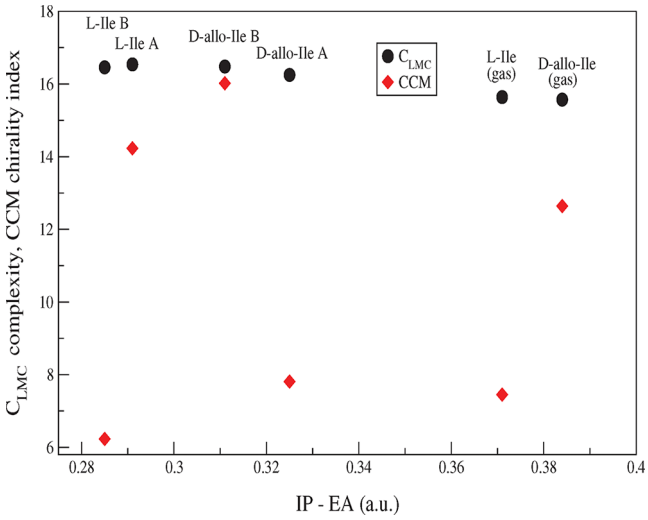


**Figure 4.** $C_{LMC}$ (López-Ruiz, Mancini, and Calbet complexity) values and CCM (continuous chirality measure) values for the different amino acids studied in this work (zwitterionic molecular units and gas phase molecules) vs IP−EA. a.u. are used for IP−EA and for $C_{LMC}$ values.

molecular units, which remarkably differ in their chirality index, while the difference in their complexities is very small. The average chirality for the two molecular units of D-allo-Ile remains higher with respect to L-Ile, in line with the findings of previous works.[88] However, interestingly, it can be noted that the complexity slightly increases in association with a gain in chirality in the protein-forming L-Ile, while for the non-proteinogenic D-allo-Ile the complexity increases and the average chirality decreases.

The observed small differences in the complexity values of L-Ile and D-allo-Ile can be expected, as the two amino acids have the same number of electrons and as the $C_{LMC}$ complexity is based on global spatial distributions. Also, by including diffuse functions in the basis set, lacking a prominent atomic character, the results can be expected not to show strong dependence on local properties of the atomic environments. Nevertheless, an increase in complexity remains when shifting from the gas phase amino acid (15.64 au for L-Ile) to the condensed phase (16.54 and 16.46 au for the two zwitterionic units of L-Ile). This means that adding Shannon entropy measures linked to the electronic properties on a (structural/geometrical) molecular complexity scale, although not enough to grasp intrinsicate properties for molecules with the same chemical formula, would help in characterizing global aspects of the electronic properties in different states of matter.

**H-Bonding Network.** The packing of both L-Ile and D-allo-Ile is clearly determined by side chains, involved in vdW's interactions, and by the charged $\alpha$-amino and $\alpha$-carboxylate groups that form H-bonds (Figure 5, visualized as $2 \times 2 \times 2$ supercells). The first type of bond gives rise to hydrophobic layers, while the second to hydrophilic layers. The H-bond patterns in the two systems are equivalent to the one reported in previous studies[70] and exhibit the same main ring motifs.[89]

The average strength of such patterns can be deduced by analyzing the energetics of intermolecular vs intramolecular stabilization or, in other words, the competition between vdW and H-bond energy. A simple but effective approach[90] can be employed in which first the contribution from vdW interactions to the binding energy of the crystal is evaluated,


DOI: 10.1021/acsearthspacechem.9b00131
ACS Earth Space Chem. 2019, 3, 1955−1965

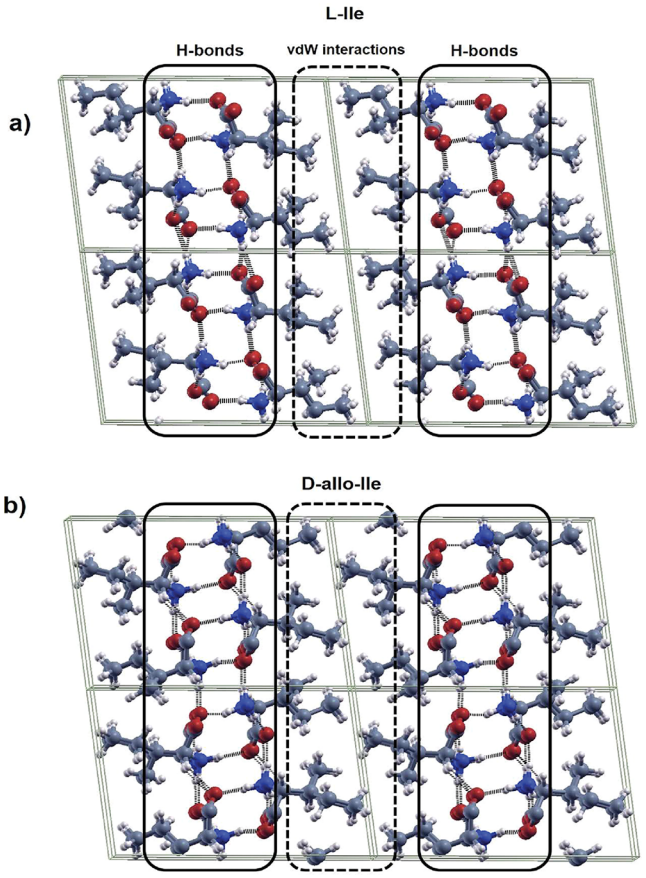


**Figure 5.** H-bond patterns in the optimized structures of (a) L-Ile and (b) D-allo-Ile. Highlighted are the hydrophobic layer, given by vdW interactions between side chains, and the hydrophilic layer given by the charged $\alpha$-amino and $\alpha$-carboxylate groups that form H-bonds.

and then the contribution from long-range electrostatic interactions and the average H-bond strength (i.e., per H-bond) are evaluated (see SI). The results show that the H-bond in D-allo-Ile is slightly stronger than the one in L-Ile, but only by a very small difference (0.4 kcal/mol), which cannot be considered as meaningful given the methods employed. The estimation should be improved via higher level approaches, first because the H-bond energy actually always includes some vdW contribution, and second because the DFT-D2 approach used here, being a pairwise-additive model of vdW interactions, ignores nonadditive many-body vdW energy contributions beyond the pairwise approximation.[91,92] If a more relevant weakness of the H-bonds pattern in L-Ile would be confirmed by more robust approaches than those considered here, such bonds could be broken more easily in a transient fashion and would allow the mobility of L-Ile molecules through a possible solvent medium.

Nevertheless, upon close inspection, a higher distortion of the pattern in D-allo-Ile can be noted: the lengths of the H-bonds formed by $\alpha$-amino and $\alpha$-carboxylate groups in the hydrophilic layers (1.74 and 1.99 Å) differ more than what occurrs in L-Ile (1.75 and 1.88 Å); the H-bond between a molecule and the one above or below in Figure 5 (i.e., within the same sheet in the hydrophobic layer) is remarkably longer in D-allo-Ile (2.33 Å) than in L-Ile (1.94 Å); also, the two bifurcated bonds differ remarkably in D-allo-Ile (2.38 and 1.78 Å), while in L-Ile they have nearly the same length (2.22 and 2.16 Å). Such slightly higher distortion of the H-bond pattern in D-allo-Ile can be expected, as the different side chain conformations of the two dissimilar molecular units in such system adapt the stacking in order to still accommodate the symmetry of the same space group as L-Ile ($P2_1$).

**Complementary Complexity Perspectives Behind Cold-Chemistry Processes.** The result that the complexity $C_{LMC}$ related to the electronic properties is higher for the amino acids in the condensed phases with respect to the gas phase molecules contrasts with the intuitive notion of "structural/geometrical" complexity of a crystalline solid. In a purely "structural/geometrical" perspective, focused on the variability of the microscopic arrangements of the components, a solid is a paradigm of simplicity, with the lowest statistical complexity. A crystalline solid is indeed a perfectly ordered system, where one specific configuration is chosen (high disequilibrium) and is made up by repetitions of elementary cells. Each of such cell requires only few bits of information to be defined (and thus "stores" only a limited amount of information). However, when looking at condensation phenomena for organic molecular systems, the smallest units relevant for electronic and chiral properties could be considered to be the single molecular units, which are not only chiral but may also have dissimilar configuration. Crystallization, like any other spontaneous process, is driven by information minimization and symmetry maximimization.[93] Different degrees of freedom in a system (configurational, vibrational, electronic/magnetic, or chiral) contribute to the total (thermodynamical, informational) entropy to different extents[49] depending on the state of matter.

It is interesting to consider, at least qualitatively, which microscopic degrees of freedom may drive the emergence of complexity in the products of different condensation (or sublimation) phenomena. Conglomerate crystals like D-allo-Ile may form significant enantiomeric excess even starting from solutions that are approximately racemic, by a process similar to stirring,[23] which might be relevant in shock-wave-driven chemistry of colliding icy grains.[17] In such reactions, it is well possible that complexity is mainly driven by the configurational degrees of freedom, rather than the chirality evolving from a nearly racemic system. Upon condensation, the average symmetry of the molecular units in D-allo-Ile increases (the zwitterionic molecular units are, on average, less chiral with respect to the gas phase amino acid). This is contrasted by the configurational contribution, as the two units are dissimilar, with the compensating side chains making the electronic density more uniformly delocalized in the unit cell (thus, with a lower disequilibrium). Racemates (as LD-Ile) display preferential crystallization/sublimation of one enantiomer[94,95] in the presence of a slight excess of one enantiomer at the start.[24] In L-Ile, the average chirality of the two zwitterionic molecular units of the condensed phase is increased with respect to the gas phase molecule. This, together with a high similarity of the two units, with no dissimilar side chains, makes the electronic density less uniformly delocalized (higher disequilibrium in both structural and electronic properties). All this suggests that the emergence of complexity in the electronic properties of organic molecules or solid organic matter may be driven by different degrees of freedom, whose relative importance is determined by the details of the formation process. Further studies are needed to disentangle the contribution of different degrees of freedom to complexity.

Interestingly, potential formation of 2-methylbutyraldehyde, a chiral Strecker precursor for the isoleucine serie, has been


DOI: 10.1021/acsearthspacechem.9b00131
ACS Earth Space Chem. 2019, 3, 1955−1965

reported in recent experiments on the effects of the interaction of energetic electrons with astrophysically relevant water/methane ices.[96] In the Solar system, Europa, Encedalus, and Titan are excellent candidates to detect organic matter in different states of matter. These bodies are subjected to cosmic rays, solar wind, and also electrons and ions from the local magnetosphere of their giant planet, with electrons penetrating deeper into the ice and triggering a rich deep-bulk chemistry. Intense ionizing radiation can produce volatiles from the solids and solid particulates from gases,[97] as relevant for Enceladus' plume, which might have and organic content as high as carbonaceous chondrites.[98]

## CONCLUSIONS

In the development of new scoring strategies of the complexity of biological molecules with respect to some universal features of life, the electronic properties of the single molecular units cannot be neglected. This work is the first investigation on the physicochemical properties of the gas and condensed phases of the amino acids of the isoleucine series, found in Antarctic meteorites with large enantiomeric excess, and on their link to complexity, chirality, and the propensity for chemical reactivity.

The results obtained show that the statistical complexity related to the electronic properties of the amino acids, as well as the inherent chirality index, could be different between the gaseous phase, as relevant, for example, in planetary/small bodies atmospheres, and the condensed phase, as relevant for formation of solid organic matter in cold chemistry processes, self-assembly, and polymerization in mineral or icy matrices at planetary/small bodies surfaces. In particular, it is found that (a) the molecular units frozen in the condensed phases have higher propensity to chemical reactivity, which suggests a potential for higher complexification of the system; (b) L-Ile, involved in protein biosynthesis, has higher propensity to chemical reactivity in both the gas and condensed phase with respect to D-allo-Ile, which is absent in living systems, gains in both complexity and chirality upon condensation, and forms a less distorted H-bond pattern.

The information theory of quantum systems offers a complementary perspective with respect to complexity notions only relying on structural/geometrical, topological properties of the molecules, or on the randomness in their arrangement in sequences. The higher complexity related to the electronic properties for the molecular units in the condensed phases contrasts with the perspective of (lowest) structural/geometrical statistical complexity of a crystalline solid (no or very little radnomness, in the arrangement of the molecular units, and high disequilibrium). The analysis presented here suggests that, while adding Shannon entropic measures related to the electronic properties to a geometry/topology-based complexity approach would not be enough to grasp intricate properties for molecules with the same chemical formula in the same state of matter, it can characterize changes in the global aspects of the electronic properties from the gas to a condensed state. Analysis of the electronic properties for several known and unknown amino acids is needed in order to define a new complexity scale based on both structural/geometrical/topological properties and on the electronic properties, with link to the propensity for chemical reactivity and charge transport.

## ASSOCIATED CONTENT

### Supporting Information

The Supporting Information is available free of charge on the ACS Publications website at DOI: 10.1021/acsearthspacechem.9b00131.

Details of the plane-wave DFT and GW calculations and of the 6-311++G(d,p) calculations; comparison with experiments for the structural parameters of the condensed phases; details on the calculations of the strength of the H-bond patterns (PDF)

## AUTHOR INFORMATION


### Corresponding Author

*E-mail: fabiana.dapieve@aeronomie.be.

### ORCID

Fabiana Da Pieve: 0000-0001-6985-9145


### Notes

The author declares no competing financial interest.

## ACKNOWLEDGMENTS

The author thanks funding from the Research Executive Agency received for a Marie Curie IEF (grant ID 627569) financed under the European Union's FP7 program, under which the work has been done, and current funding from the Research Executive Agency under the European Union's Horizon 2020 Research and Innovation program (grant ID 776410), under which the work has been submitted.

## REFERENCES


(1) Dundas, C. M.; Bramson, A. M.; Ojha, L.; Wray, J. J.; Mellon, M. T.; Byrne, S.; McEwen, A. S.; Putzig, N. E.; Viola, D.; Sutton, S.; Clark, E.; Holt, J. W. Exposed subsurface ice sheets in the Martian mid-latitudes. *Science* **2018**, *359*, 199−201.

(2) Soderlund, K. M.; Schmidt, B. E.; Wicht, J.; Blankenship, D. D. Ocean driven heating of Europa's icy shell at low latitudes. *Nat. Geosci.* **2014**, *7*, 16−19.

(3) Waite, J. H.; Glein, C. R.; Perryman, R. S.; Teolis, B. D.; Magee, B. A.; Miller, G.; Grimes, J.; Perry, M. E.; Miller, K. E.; Bouquet, A.; Lunine, J. I.; Brockwell, T.; Bolton, S. J. Cassini finds molecular hydrogen in the Enceladus plume: evidence for hydrothermal processes. *Science* **2017**, *356*, 155−159.

(4) Vago, J. L.; Westall, F. Pasteur Instrument Teams, Landing Site Selection Working Group, and Other Contributors. Habitability on early Mars and the search for biosignatures with the ExoMars rover. *Astrobiology* **2017**, *17*, 471−501.

(5) Cleaves, J. H., II; Neish, C.; Callahan, M. P.; Parker, E.; Fernández, F. M.; Dworkin, J. P. Amino acids generated from hydrated Titan tholins: Comparison with Miller-Urey electric discharge products. *Icarus* **2014**, *237*, 182−189.

(6) Cable, M. L.; Vu, T. H.; Maynard-Casely, H. E.; Choukroun, M.; Hodyss, R. The acetylene-ammonia co-crystal on Titan. *ACS Earth Space Chem.* **2018**, *2*, 366−375.

(7) Hörst, S. M.; Yelle, R. V.; Buch, A.; Carrasco, N.; Cernogora, G.; Dutuit, O.; Quirico, E.; Sciamma-O'Brien, E.; Smith, M. A.; Somogyi, A.; Szopa, C.; Thissen, R.; Vuitton, V. Formation of amino acids and nucleotide bases in a Titan atmosphere simulation experiment. *Astrobiology* **2012**, *12*, 809−17.

(8) Bergantini, A.; Pilling, S.; Nair, B. G.; Mason, N. J.; Fraser, H. J. Processing of analogues of plume fallout in cold regions of Encedalus by energetic electrons. *Astron. Astrophys.* **2014**, *570*, A120.

(9) Guzman, M.; Lorenz, R.; Hurley, D.; Farrell, W.; Spencer, J.; Hansen, C.; Hurford, T.; Ibea, J.; Carlson, P.; McKay, C. P. Collecting amino acids in the Enceladus plume. *Int. J. Astrobiol.* **2019**, *18*, 1−13.




DOI: 10.1021/acsearthspacechem.9b00131
*ACS Earth Space Chem.* 2019, 3, 1955−1965

(10) Postberg, F.; Khawaja, N.; Abel, B.; Choblet, G.; Glein, C. R.; Gudipati, M. S.; Henderson, B. L.; Hsu, H.-W.; Kempf, S.; Klenner, F.; Moragas-Klostermeyer, G.; Magee, B.; Nölle, L.; Perry, M.; Reviol, R.; Schmidt, J.; Srama, R.; Stolz, F.; Tobie, G.; Trieloff, M.; Waite, J. H. Macromolecular organic compounds from the depths of Enceladus. *Nature* **2018**, *558*, 564−568.
(11) Butscher, T.; Duvernay, F.; Danger, G.; Chiavassa, T. Radical-induced chemistry from VUV photolysis of interstellar ice analogues containing formaldehyde. *Astron. Astrophys.* **2016**, *593*, A60.
(12) de Barros, A. L. F.; da Silveira, E. F.; Fulvio, D.; Rothard, H.; Boduch, P. Ion irradiation of ethane and water mixture ice at 15 K: Implications for the solar system and the ISM. *ApJ.* **2016**, *824*, 81.
(13) Shingledecker, C. N.; Tennis, J.; Le Gal, R.; Herbst, E. On cosmic-ray-driven grain chemistry in cold core models. *ApJ.* **2018**, *861*, 20.
(14) Ciesla, F. J.; Sandford, S. A. Organic synthesis via irradiation and warming of ice grains in the solar nebula. *Science* **2012**, *336*, 452−454.
(15) Altwegg, K.; Balsiger, H.; Bar-Nun, A.; Berthelier, J.-J.; Bieler, A.; Bochsler, P.; Briois, C.; Calmonte, U.; Combi, M. R.; Cottin, H.; De Keyser, J.; Dhooghe, F.; Fiethe, B.; Fuselier, S. A.; Gasc, S.; Gombosi, T. I.; Hansen, K. C.; Haessig, M.; Jäckel, A.; Kopp, E.; Korth, A.; Le Roy, L.; Mall, U.; Marty, B.; Mousis, O.; Owen, T.; Rème, H.; Rubin, M.; Sémon, T.; Tzou, C. Y.; Hunter Waite, J.; Wurz, P. Prebiotic chemicals - amino acids and phosphorus - in the coma of comet 67P/Churyumov-Gerasimenko. *Science Advances* **2016**, *2* (5), No. e1600285.
(16) Vasyunin, A. I.; Herbst, E. A unified Monte Carlo treatment of gas phase chemistry for large reaction networks. II. A multiphase gas-surface layered-bulk model. *Astrophys. J.* **2013**, *762*, 86.
(17) Cassone, G.; Franz Saija, F.; Sponer, J.; Sponer, J. E.; Ferus, M.; Krus, M.; Ciaravella, A.; Jiménez-Escobar, A.; Cecchi-Pestellini, C. Dust motions in magnetized turbulence: source of chemical complexity. *Astrophys. J., Lett.* **2018**, *866*, L23.
(18) Pizzarello, S.; Schrader, D. L.; Monroe, A. A.; Lauretta, D. S. Large enantiomeric excesses in primitive meteorites and the diverse effects of water in cosmochemical evolution. *Proc. Natl. Acad. Sci. U. S. A.* **2012**, *109*, 11949−11954.
(19) Cronin, J. R.; Pizzarello, S. Enantiomeric excesses in meteoritic amino acids. *Science* **1997**, *275*, 951−955.
(20) McGuire, B. A.; Carroll, P. B.; Loomis, R. A.; Finneran, I. A.; Jewell, P. R.; Remijan, A. J.; Blake, G. A. Discovery of the interstellar chiral molecule propylene oxide ($CH_3CHCH_2O$). *Science* **2016**, *352*, 1449−1452.
(21) Myrgorodska, I.; Meinert, C.; Martins, Z.; Le Sergeant d'Hendecourt, L.; Meierhenrich, U. J. Molecular chirality in meteorites and interstellar ices, and the chirality experiment on board the ESA cometary Rosetta mission. *Angew. Chem., Int. Ed.* **2015**, *54*, 1402−12.
(22) Viedma, C. Chiral symmetry breaking during crystallization: complete chiral purity induced by nonlinear autocatalysis and recycling. *Phys. Rev. Lett.* **2005**, *94*, 065504.
(23) Viedma, C.; Ortiz, J. E.; de Torres, T.; Izumi, T.; Blackmond, D. G. Evolution of solid phase homochirality for a proteinogenic amino acid. *J. Am. Chem. Soc.* **2008**, *130*, 15274−15275.
(24) Blackmond, D. G.; Klussmann, M. Spoilt for choices: assessing phase behavior model for the evolution of homochirality. *Chem. Commun.* **2007**, 3990−3996.
(25) Steendam, R. R. E.; Verkade, J. M. M.; van Benthem, T. J. B.; Meekes, H.; van Enckevort, W. J. P.; Raap, J.; Rutjes, F. P. J. T.; Vlieg, E. Emergence of single-molecular chirality from achiral reactants. *Nat. Commun.* **2014**, *5*, 5543.
(26) Sephton, M. A. Organic compounds in carbonaceous meteorites. *Nat. Prod. Rep.* **2002**, *19*, 292−311.
(27) Cronin, J. R.; Pizzarello, S. Amino acids in meteorites. *Adv. Space Res.* **1983**, *3*, 5−18.
(28) Cronin, J. R.; Chang, S. Organic matter in meteorites: molecular and isotopic analyses of the Murchison meteorite. *The Chemistry of Life's Origin*; Greenberg, J. M., Mendoza-Gomez, C. X., Pirronello, V., Eds.; Kluwer: Dordrecht, The Netherlands, 1993; pp 209−258.
(29) Botta, O.; Bada, J. L. Extraterrestrial organic compounds in meteorites. *Surv. Geophys.* **2002**, *23*, 411−467.
(30) Walker, S. I.; Bains, W.; Cronin, L.; DasSarma, S.; Danielache, S.; Domagal-Goldman, S.; Kacar, B.; Kiang, N. Y.; Lenardic, A.; Reinhard, C. T.; Moore, W.; Schwieterman, E. W.; Shkolnik, E. L.; Smithz, H. B. Exoplanet Biosignatures: Future Directions. *Astrobiology* **2018**, *18*, 779−824.
(31) Johnson, S. S.; Anslyn, E. V.; Graham, H. V.; Mahaffy, P. R.; Ellington, A. D. Fingerprinting Non-Terran Biosignatures. *Astrobiology* **2018**, *18*, 915−922.
(32) Böttcher, T. From molecules to life: quantifying the complexity of chemical and biological systems in the Universe. *J. Mol. Evol.* **2018**, *86*, 1−10.
(33) Böttcher, T. An additive definition of molecular complexity. *J. Chem. Inf. Model.* **2016**, *56*, 462−470.
(34) Shannon, C. E.; Weaver, W. *The Mathematical Theory of Communication*; Illini Books: Chicago, IL, 1963.
(35) Ilardo, M.; Meringer, M.; Freeland, S.; Rasulev, B.; Cleaves, J. J. Extraordinarily adaptive properties of the genetically encoded amino acids. *Sci. Rep.* **2015**, *5*, 9414.
(36) Adam, Z. R.; Zubarev, D.; Aono, M.; Cleaves, H. J. Subsumed complexity: abiogenesis as a by-product of complex energy transduction. *Philos. Trans. R. Soc., A* **2017**, *375*, 20160348.
(37) England, J. Dissipative adaptation in driven self-assembly. *Nat. Nanotechnol.* **2015**, *10*, 919.
(38) Vattay, G.; Salahub, D.; Csabai, I.; Nassimi, A.; Kaufmann, S. A. Quantum criticality at the origin of life. *J. Phys.: Conf. Ser.* **2015**, *626*, 012023 and refs therein .
(39) Vattay, G.; Kauffman, S.; Niiranen, S. Quantum biology on the edge of quantum chaos. *PLoS One* **2014**, *9*, No. e89017.
(40) Granold, M.; Hajieva, P.; Tos, M. I.; Irimie, F.-D.; Moosmann, B. Modern diversification of the amino acid repertoire driven by oxygen. *Proc. Natl. Acad. Sci. U. S. A.* **2018**, *115*, 41−46.
(41) Vladilo, G.; Hassanali, A. Hydrogen bonds and life in the Universe. *Life* **2018**, *8*, 1.
(42) Esquivel, R. O.; Molina-Espíritu, M.; Salas, F.; Soriano, C.; Barrientos, C.; Dehesa, J. S.; Dobado, J. Decoding the building blocks of life from the perspective of quantum information. In *Advances in Quantum Mechanics*; INTECH Open Access Publisher, 2013.
(43) Esquivel, R. O.; Molina-Espíritu, M.; López-Rosa, S.; Soriano-Correa, C.; Barrientos-Salcedo, C.; Kohout, M.; Dehesa, J. S. Predominant information quality scheme for the essential amino acids: an information-theoretical analysis. *ChemPhysChem* **2015**, *16*, 2571−81.
(44) López-Ruiz, R.; Mancini, H. L.; Calbet, X. A statistical measure of complexity. *Phys. Lett. A* **1995**, *209*, 321−326.
(45) Shiner, J.; Davison, M.; Landsberg, P. Simple measure for complexity. *Phys. Rev. E: Stat. Phys., Plasmas, Fluids, Relat. Interdiscip. Top.* **1999**, *59*, 1459−1464.
(46) Borgoo, A.; Godefroid, M.; Sen, K. D.; De Proft, F.; Geerlings, P. Quantum similarity of atoms: a numerical Hartree-Fock and Information Theory approach. *Chem. Phys. Lett.* **2004**, *399*, 363−367.
(47) Janssens, S.; Bultinck, P.; Borgoo, A.; Van Alsenoy, C.; Geerlings, P. Alternative Kullback-Leibler information entropy for enantiomers. *J. Phys. Chem. A* **2010**, *114*, 640−645.
(48) Bultinck, P.; Carbó-Dorca, R. Molecular quantum similarity using conceptual DFT descriptors. *Proc. - Indian Acad. Sci., Chem. Sci.* **2005**, *117*, 425−435.
(49) Krivovichev, S. V. Structural complexity and configurational entropy of crystals. *Acta Crystallogr., Sect. B: Struct. Sci., Cryst. Eng. Mater.* **2016**, *B72*, 274−276.
(50) Bada, J. L.; Zhao, M.; Steinberg, S.; Ruth, E. Isoleucine stereoisomers on the Earth. *Nature* **1986**, *319*, 314−316.
(51) Dalhus, B.; Görbitz, C. H. Structural relationships in crystals accommodating different stereoisomers of 2-amino-3-methylpentanoic acid. *Acta Crystallogr., Sect. B: Struct. Sci.* **2000**, *B56*, 720−727.


DOI: 10.1021/acsearthspacechem.9b00131
*ACS Earth Space Chem.* 2019, 3, 1955−1965

(52) Day, G. M.; Cooper, T. G. Crystal packing predictions of the α-amino acids: methods assessment and structural observations. *CrystEngComm* **2010**, *12*, 2443−2453.
(53) Görbitz, C. H.; Dalhus, B. L-Isoleucine, redetermination at 120K. *Acta Crystallogr., Sect. C: Cryst. Struct. Commun.* **1996**, *52*, 1464.
(54) Becke, A. D. Density functional thermochemistry. III. The role of exact exchange. *J. Chem. Phys.* **1993**, *98*, 5648−5652.
(55) Lee, C.; Yang, W.; Parr, R. G. Development of the Colle-Salvetti correlation-energy formula into a functional of the electron density. *Phys. Rev. B: Condens. Matter Mater. Phys.* **1988**, *37*, 785−789.
(56) Kresse, G.; Furthmüller, J. Efficient iterative schemes for ab initio total-energy calculations using a plane-wave basis set. *Phys. Rev. B: Condens. Matter Mater. Phys.* **1996**, *54*, 11169.
(57) Kresse, G.; Joubert, D. From ultrasoft pseudopotentials to the projector augmented-wave method. *Phys. Rev. B: Condens. Matter Mater. Phys.* **1999**, *59*, 1758.
(58) Perdew, J. P.; Burke, K.; Ernzerhof, M. Generalized gradient approximation made simple. *Phys. Rev. Lett.* **1996**, *77*, 3865.
(59) Grimme, S. Semiempirical GGA-type density functional constructed with a long-range dispersion correction. *J. Comput. Chem.* **2006**, *27*, 1787−1799.
(60) Frisch, M. J.; Trucks, G. W.; Schlegelet, H. B.; et al. *Gaussian 09*, revision D.01; Gaussian Inc.: Wallingford, CT, 2009.
(61) Cossi, M.; Rega, N.; Scalmani, G.; Barone, V. New developments in the polarizable continuum model for quantum mechanical and classical calculations on molecules in solution. *J. Chem. Phys.* **2002**, *117*, 43.
(62) Parr, R. G.; Pearson, R. G. Absolute hardness: companion parameter to absolute electronegativity. *J. Am. Chem. Soc.* **1983**, *105*, 7512−7575.
(63) Zhan, C.-G.; Nichols, J. A.; Dixon, D. A. Ionization potential, electron affinity, electronegativity, hardness, and electron excitation energy: molecular properties from Density Functional Theory orbital energies. *J. Phys. Chem. A* **2003**, *107*, 4184.
(64) López-Ruiz, R.; Mancini, H. L.; Calbet, X. A statistical measure of complexity. *Phys. Lett. A* **1995**, *209*, 321−326.
(65) Petz, D. *Quantum Information Theory and Quantum Statistics*; Springer: Berlin Heidelberg, 2008.
(66) Berntsen, J.; Espelid, T. O.; Genz, A. Algorithm 698: Dcuhre: an adaptive multidemensional integration routine for a vector of integrals. *ACM Trans. Math. Softw.* **1991**, *17*, 452−456.
(67) Van Alsenoy, C.; Peeters, A. Brabo: a program for ab initio studies on large molecular systems. *J. Mol. Struct.: THEOCHEM* **1993**, *286*, 19.
(68) Zayit, A.; Pinsky, M.; Elgavi, H.; Dryzun, C.; Avnir, D. A web site for calculating the degree of chirality. *Chirality* **2001**, *23*, 17−23.
(69) Görbitz, C. H.; Vestli, K.; Orlando, R. A solution to the observed Z = 2 preference in the crystal structures of hydrophobic amino acids. *Acta Crystallogr., Sect. B: Struct. Sci.* **2009**, *B65*, 393−400.
(70) Varughese, K. I.; Srinivasan, R. Studies in molecular structure, symmetry and conformation XII: Crystal and molecular structure of D-alloisoleucine. *J. Cryst. Mol. Struct.* **1975**, *5*, 317.
(71) Chaban, G. M.; Pizzarello, S. Ab initio calculations of 6- and 7-carbon meteoritic amino acids and their diastereomers. *Meteoritics and Planetary Science* **2010**, *45*, 1053−1060.
(72) Close, D. M. Calculated Vertical Ionization energies of the common α-amino acids in the gas phase and in solution. *J. Phys. Chem. A* **2011**, *115*, 2900−2912.
(73) Millefiori, S.; Alparone, A.; Millefiori, A.; Vanella, A. Electronic and vibrational polarizabilities of the twenty naturally occurring amino acids. *Biophys. Chem.* **2008**, *132*, 139.
(74) Papp, P.; Shchukin, P.; Kočíšek, J.; Matejčík, Š. Electron ionization and dissociation of aliphatic amino acids. *J. Chem. Phys.* **2012**, *137*, 105101.
(75) Lesarri, A.; Sánchez, R.; Cocinero, E.; et al. Coded amino acids in gas phase: the shape of isoleucine. *J. Am. Chem. Soc.* **2005**, *127*, 12952.
(76) Dehareng, D.; Dive, G. Vertical ionization energies of α-L-amino acids as a function of their conformation: an ab initio study. *Int. J. Mol. Sci.* **2004**, *5*, 301−332.
(77) Ganesan, A.; Brunger, M. J.; Wang, F. A study of aliphatic amino acids using simulated vibrational circular dichroism and Raman optical activity spectra. *Eur. Phys. J. D* **2013**, *67*, 229.
(78) Tulip, P. R.; Clark, S. J. Structural and electronic properties of L-amino acids. *Phys. Rev. B: Condens. Matter Mater. Phys.* **2005**, *71*, 195117.
(79) Da Pieve, F.; Avendaño-Franco, G.; De Proft, F.; Geerlings, P. Interstellar condensed (icy) amino acids and precursors: theoretical absorption and circular dichroism under UV and soft X-ray irradiation. *Mon. Not. R. Astron. Soc.* **2014**, *440*, 494−503.
(80) Silva, A. M.; Silva, B. P.; Sales, F. A. M.; Fireire, V. N.; Moreira, E.; Fulco, U. L.; Albuquerque, E. L.; Maia, F. F., Jr.; Caetano, E. W. S. Optical absorption and DFT calculations in L-aspartic acid anhydrous crystals: Charge carrier effective masses point to semiconducting behavior. *Phys. Rev. B: Condens. Matter Mater. Phys.* **2012**, *86*, 195201.
(81) Gavezzotti, A. Structure and intermolecular potentials in molecular crystals. *Modell. Simul. Mater. Sci. Eng.* **2002**, *10*, R1.
(82) Caetano, E. W. S.; Pinheiro, J. R.; Zimmer, M.; Freire, V. N.; Farias, G. A.; Bezerra, G. A.; Cavada, B. S.; Fernadez, J. R. L.; Leite, J. R.; de Oliveira, M. C. F.; Pinheiro, J. A.; de Lima Filho, J. L.; Leite Alves, H. W. Molecular signature in the photoluminescence of α-glycine, L-alanine and L-asparagine crystals: detection, ab initio calculations, and bio-sensor applications. In *Proceedings of the 27th International Conference on the Physics of Semiconductors*; Menendez, J., Van de Walle, C., Eds.; AIP Conf. Proc. No. 772; AIP, New York, 2005; p 1095.
(83) Flores, M. Z. S.; Freire, V. N.; dos Santos, R. P.; Farias, G. A.; Caetano, E. W. S.; de Oliveira, M. C. F.; Fernandez, J. L. R.; Scolfaro, L. M. R.; Bezerra, M. J. B.; Oliveira, T. M.; Bezerra, G. A.; Cavada, B. S.; Leite Alves, H. W. Optical absorption and electronic band structure first-principles calculations of α-glycine crystals. *Phys. Rev. B: Condens. Matter Mater. Phys.* **2008**, *77*, 115104.
(84) Klasinc, L. Application of photoelectron spectroscopy to biologically active molecules and their constituent parts: III. Amino acids. *J. Electron Spectrosc. Relat. Phenom.* **1976**, *8*, 161.
(85) Abreu, N. M.; Brearley, A. J. Early solar system processes recorded in the matrices of two highly pristine CR3 carbonaceous chondrites, MET 00426 and QUE 99177. *Geochim. Cosmochim. Acta* **2010**, *74*, 1146−1171.
(86) Pruneda, J. M.; Sánchez-Portal; Arnau, A.; Juaristi, J. I.; Artacho, E. Electronic stopping power from first principles. *Phys. Rev. Lett.* **2007**, *99*, 235501−235504.
(87) Amovilli, C.; Floris, F. Shannon entropy in atoms: a test for the assessment of density functionals in Kohn-Sham theory. *Computation* **2018**, *6*, 36−42.
(88) Jamróz, M. H.; Rode, J. E.; Ostrowski, S.; Lipiński, P. F.; Dobrowolski, J.Cz. Chirality measures of α-amino acids. *J. Chem. Inf. Model.* **2012**, *52*, 1462−1479.
(89) Fábián, L.; Chisholm, J. A.; Galek, P. T. A.; Samuel Motherwell, W. D.; Feeder, N. Hydrogen-bond motifs in the crystals of hydrophobic amino acids. *Acta Crystallogr., Sect. B: Struct. Sci.* **2008**, *B64*, 504−514.
(90) Zucca, R.; Boero, M.; Massobrio, C.; Molteni, C.; Cleri, F. Interacting Lewis-X carbohydrates in condensed phase: a first-principles molecular dynamics study. *J. Phys. Chem. B* **2011**, *115*, 12599−12606.
(91) Reilly, A. M.; Tkatchenko, A. van der Waals dispersion interactions in molecular materials: beyond pairwise additivity. *Chem. Sci.* **2015**, *6*, 3289−3301.
(92) Tkatchenko, A. Current understanding of Van der Waals effects in realistic materials. *Adv. Funct. Mater.* **2015**, *25*, 2054−2061.
(93) Lin, S. K. The nature of the chemical process 1. Symmetry evolution -revised information. *J. Chem. Inf. Comput. Sci.* **1996**, *36*, 367.


DOI: 10.1021/acsearthspacechem.9b00131
*ACS Earth Space Chem.* 2019, 3, 1955−1965

(94) Fletcher, S. P.; Jagt, R. B. C.; Feringa, B. L. An astrophysically relevant mechanism for amino acid enantiomer enrichment. *Chem. Commun.* **2007**, 2578−2580.
(95) Tarasevych, A. V.; Sorochinsky, A. E.; Kukhar, V. P.; Guillemin, J.-C. Deracemization of amino acids by partial sublimation and via homochiral self-organization. *Origins Life Evol. Biospheres* **2013**, *43*, 129−135.
(96) Bergantini, A.; Maksyutenko, P.; Kaiser, R. I. On the formation of the $C_2H_{6O}$ isomers ethanol ($C_2H_5OH$) and dimethyl ether ($CH_3OCH_3$) in star-forming regions. *ApJ.* **2017**, *841*, 96−120.
(97) Khare, B. N.; Bakes, E. L. O.; Cruikshank, D.; McKay, C. P. Solid organic matter in the atmosphere and on the surface of outer Solar System bodies. *Adv. Space Res.* **2001**, *27*, 299−307.
(98) Steel, E. L.; Davila, A.; McKay, C. P. Abiotic and biotic formation of amino acids in the Enceladus ocean. *Astrobiology* **2017**, *17*, 862−875.



DOI: 10.1021/acsearthspacechem.9b00131
*ACS Earth Space Chem.* 2019, 3, 1955−1965